CHEMISTRY
A EUROPEAN JOURNAL

DOI: 10.1002/chem.200500587

Numerical Simulation of the Effect of Solvent Viscosity on the Motions of a β-Peptide Heptamer

Peter J. Gee and Wilfred F. van Gunsteren*[a]

Abstract: This report examines the effect of a decrease in solvent viscosity on the simulated folding behaviour of a β-peptide heptamer in methanol. Simulations of the molecular dynamics of the heptamer H-β^3-HVal-β^3-HAla-β^3-HLeu-(*S*,*S*)-β^3-HAla(αMe)-β^3-HVal-β^3-HAla-β^3-HLeu-OH in methanol, with an explicit representation of the methanol molecules, were performed for 80 ns at various solvent viscosities. The simulations indicate that at a solvent viscosity of one third of that of methanol, only the dynamic aspects of the folding process are altered, and that the rate of folding is increased. At a viscosity of one tenth of that of methanol, insufficient statistics are obtained within the 80 ns period. We suggest that 80 ns is an insufficient time to reach conformational equilibrium at very low viscosity because the dependence of the folding rate of a β-peptide on solvent viscosity has two regimes; a result that was observed in another computational study for α-peptides.

Keywords: computer chemistry · molecular dynamics · peptides · protein folding · solvent viscosity

Introduction

The dynamic behaviour of a solvated peptidic polymer is determined, in part, by the physical properties of the medium in which it moves; one such property is the solvent viscosity. The effect of a change in viscosity on the dynamics of a helix-forming β-peptide heptamer H-β^3-HVal-β^3-HAla-β^3-HLeu-(*S*,*S*)-β^3-HAla(αMe)-β^3-HVal-β^3-HAla-β^3-HLeu-OH (Figure 1) is the subject of this report. The dynamics of the molecule, with methanol as the solvent, were simulated for 80 ns in atomic detail, with an explicit representation of the solvent molecules, at a series of viscosities. The resulting motions are compared herein.

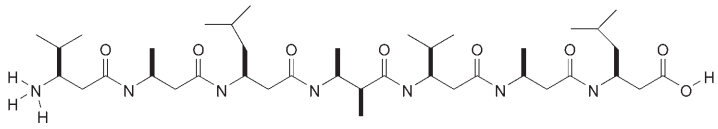

Figure 1. β-Peptide heptamer whose motions were simulated.

[a] Dr. P. J. Gee, Prof. Dr. W. F. van Gunsteren
Laboratory of Physical Chemistry
Swiss Federal Institute of Technology
8093 Zürich (Switzerland)
Fax: (+41) 632-1039
E-mail: wfvgn@igc.phys.chem.ethz.ch

For the investigation of the effects of viscosity changes on a physico-chemical process, computational methods have two advantages over experimental approaches. Firstly, very low viscosities can be simulated. Secondly, and more importantly, the viscosity of the solvent can be varied without changing other (non-dynamic) properties of the solvent and, more especially, solute–solvent interactions. This is difficult to do experimentally: co-solvents are added to the solution under investigation and these tend to influence the conformational behaviour of the solute through both their molecular size and the interactions they have with the solvent and the solute—and the effect can be sizeable.[1] A simple way to vary the viscosity in a molecular simulation is to change the mass of each solvent molecule by a certain scaling factor:[2] if the factor is denoted *S*, then the change in viscosity of the solvent on scaling of the molecular masses would be $\sqrt{S}$.[3,4] This procedure does not affect the size of the solvent molecules and does not change properties of the solvent that are not dynamic in nature; it is the method employed here.

A previous report on a similar theme[5] suggested that the dependence of the folding rate of a 20-residue α-polypeptide on viscosity, simulated by using an implicit solvation model, has two regimes: at viscosities as low as one tenth of the viscosity of water, a linear dependence is observed; at even lower viscosities, a power-law dependence is observed, with exponent −0.2. The present report may be considered in relation to these results, though two differences in approach

must be noted: firstly, the simulations reported here used an explicit representation of the solvent molecules (the relative merits of an implicit versus an explicit representation are the subject of ongoing debate); secondly, the sampling of the statistical mechanics of the system under study was comparatively limited: simulations in which solvent molecules are explicit are computationally expensive.

The peptide whose motions were simulated is shown in Figure 1. Experimentally, it is associated with a 3_1-helical fold,[6] and this helix is the most populated conformation in numerical simulations of the molecule.[7] The peptide solvated in methanol was simulated at 340 K and 1 atm over 80 ns for three different solvent viscosities: the natural viscosity of the methanol model used (η_n), and one third (η_{low}) and one tenth (η_{vlow}) of this viscosity. The temperature chosen approximated the melting temperature of the helix to maximise the number of (un)folding events.

Results

Figure 2 shows the time courses of the number of conformational clusters of the three simulations, each of which is characterised by a different solvent viscosity. By taking the total number of conformational clusters at each time point into account (Figure 2 top panel) it is evident that conformational sampling does not converge to a constant value in the simulation at viscosity η_{vlow}, and that there is also a slight drift in the other simulations. However, the contribution to the total of "artificial" clusters, which has very few members, is large, and by discounting such clusters (Figure 2 bottom panel), the drift in conformational sampling in all cases is much less pronounced. From the time courses of the backbone atom-positional root-mean-square deviation (RMSD) of the trajectory structures from the helical NMR model conformation (Figure 3), it is clear that in all runs, the folded conformation is sampled and that a number of folding–unfolding events are observed. The most populated conformations of each simulation are shown in Figure 4. Structurally, they are more or less the same: the most populated conformation has an atom-positional RMSD of 0.06 nm from the helical NMR model conformation; the second-ranked conformation has a RMSD of 0.22 nm at normal solvent viscosity and 0.23 nm at low and very low solvent viscosities; a similar value characterises the third most frequent conformation (0.21 nm for simulation η_n; 0.19 for η_{low}; 0.18 for η_{vlow}). The simulations differ in the time spent in the different conformations (Table 1). At normal or low solvent viscosity, the statistical weight of the most-populated conformations is similar, but at very low solvent viscosity, the helical conformation—the first-ranked conformation—is more populated and comprises around 60% of the 80 ns trajectory. Statistics describing residence in the folded conformation in each of the simulations also reflect this: the total residence time in the folded conformation is largest at very low solvent viscosity.

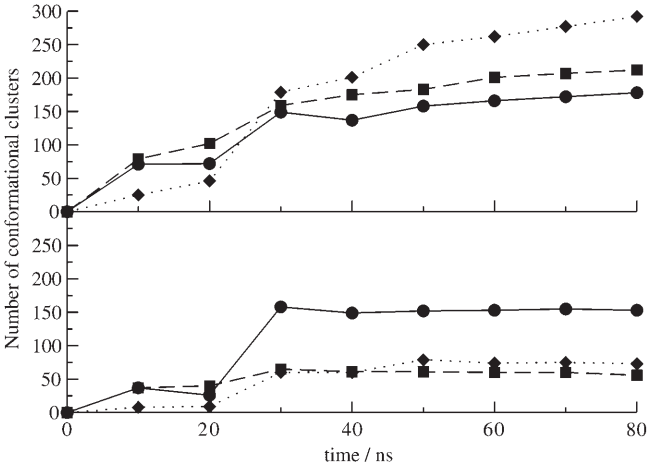

Figure 2. Time courses of the number of conformational clusters of the β-heptapeptide shown in Figure 1 in solvents that differ in only their viscous properties: normal solvent viscosity η_n (●); solvent viscosity $\eta_{low} = {}^1/_3\eta_n$ (■); solvent viscosity $\eta_{vlow} = {}^1/_{10}\eta_n$ (◆). Each point in the curves of the upper panel represents the total number of conformational clusters at the corresponding time point. In the lower panel, each point represents the number of conformational clusters that make up 95% of the trajectory sampled at the corresponding time point. For a definition of a cluster, see the Experimental Section.

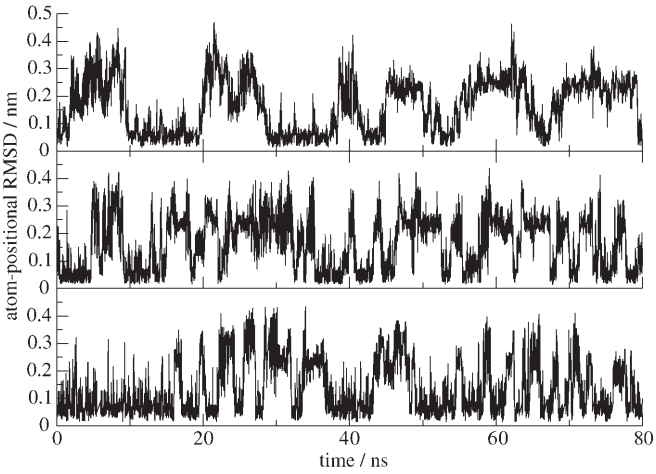

Figure 3. Time course of the backbone atom-positional root-mean-square deviation (RMSD) from the NMR-derived 3_1-helical model conformation of the backbone atoms of internal residues of the β-heptapeptide of Figure 1 in solvents that differ in only their viscous properties: top, normal solvent viscosity η_n; middle, solvent viscosity $\eta_{low} = {}^1/_3\eta_n$; bottom, solvent viscosity $\eta_{vlow} = {}^1/_{10}\eta_n$.

Discussion and Conclusion

The equilibrium properties of the simulation at very low solvent viscosity differ from those of the other two simulations. A change in the viscosity of a solvent is expected to alter the molecular dynamics of a solute molecule, and to leave the non-dynamic characteristics of any conformational equi-

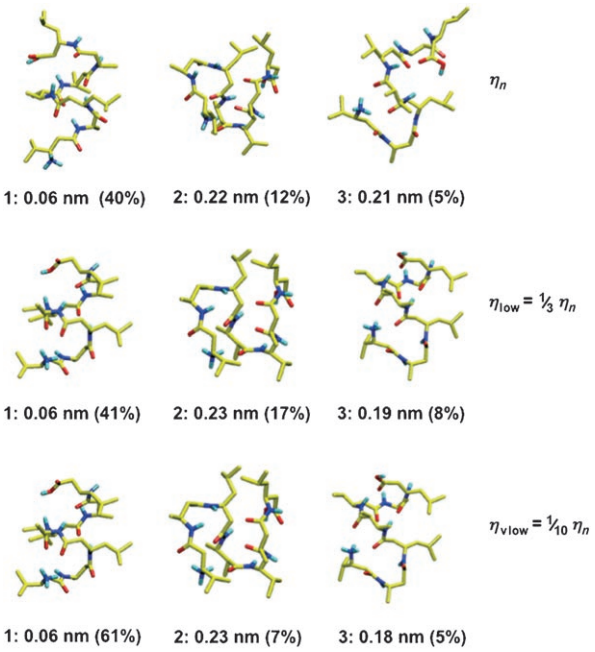

Figure 4. Central member configurations of the three top-ranked conformational clusters of the β-heptapeptide of Figure 1 at 340 K and at different solvent viscosities: top, normal solvent viscosity η_n; middle, solvent viscosity $\eta_{low} = {}^1/_3\eta_n$; bottom, solvent viscosity $\eta v_{low} = {}^1/_{10}\eta_n$. The numbers below each configuration show the rank of the conformational cluster represented by the configuration (left); the atom-positional root-mean-square deviation from the NMR-derived 3_1-helical conformation of the backbone atoms of internal residues (middle); and the percentage of the trajectory population that falls into the cluster represented. In each case, the sample trajectory is 80 ns.

Table 1. Thermodynamic and dynamic characteristics of the "folding–unfolding" equilibrium at different solvent viscosities. The margin of error shown is derived from the assumption that the folding events are Poisson distributed. At moderate to high intensities, a Poisson distribution is approximated by a normal distribution with standard deviation $(\text{intensity})^{0.5}$. Here, the intensity is the number of folding events, and the margin of error shown is the square root of that number.

Solvent viscosity	η_n	$\eta_{low} = {}^1/_3\eta_n$	$\eta_{vlow} = {}^1/_{10}\ \eta_n$
Number of folding events	92 ± 10	137 ± 12	127 ± 11
Total residence time [ps]	28150 ± 3097	29670 ± 2670	41320 ± 3719
Mean residence time [ps]	306 ± 34	217 ± 20	325 ± 29
Fraction folded	0.35 ± 0.04	0.37 ± 0.03	0.52 ± 0.05
Equilibrium constant	1.8 ± 0.2	1.7 ± 0.15	0.9 ± 0.08
Estimated free energy of folding [kJ mol^{-1}]	1.7 ± 0.2	1.5 ± 0.14	-0.2 ± 0.02

libria unchanged. In the limit of perfect sampling, one would, therefore, expect that the "folding–unfolding" equilibrium of all the simulations would have the same non-dynamic, equilibrium characteristics, and that only the mean residence time would possibly change as the viscosity of the solvent is lowered. This is clearly observed if the viscosity is decreased by a factor of one third; it does not happen if the viscosity is lowered to one tenth of that of the reference run.

This anomaly may be attributed to limited statistical sampling. At 80 ns, the conformational distribution at very low solvent viscosity is still not close to that characteristic of the "folding–unfolding" equilibrium at normal solvent viscosity in methanol. Although this is inconvenient, it may be significant. As was noted in the introduction, results of another simulation study,[5] in which more powerful computational resources were used to estimate rates of folding from multiple long-time trajectories, revealed that there may be two viscosity regimes associated with the folding of the Tryptophan Cage polypeptide, a small protein, in waterlike solvents. The first regime applies for viscosities ranging from that of water to just above one tenth of this viscosity; within this range, the rate of folding shows a more or less linear dependence on solvent viscosity and can be explained by the theoretical model proposed by Kramers.[8] The second regime occurs at lower values of viscosity, at which the rate of folding shows an inverse power-law dependence on solvent viscosity, with an exponent of around one fifth, and can no longer be explained by Kramers' model. It may be that the slower approach to the folding equilibrium at η_{vlow} is indicative of a similar difference in response for the β-peptide. From the current data, no more than this tentative suggestion can be made, and a more extensive examination of the viscosity response would be needed. However, in view of the computational expense of explicit solvent simulations with a reduced time-step, faster computers are required before such studies can be undertaken. Nevertheless, at an approximately normal solvent viscosity of the methanol solvent the rate of folding seems to be governed by solvent viscosity, and not by intrasolute interactions. This implies that non-dynamic equilibrium properties of solvated peptides can be studied more efficiently by artificially lowering the solvent viscosity in molecular dynamics simulations.

Experimental Section

Simulation set-up: The data presented in this report are derived from three 80 ns molecular dynamics simulations. The initial 50 ns of one of these simulations (at normal solvent viscosity) was the subject of an earlier report.[7] The simulations were performed by using the GROMOS96 package of programs[9,10] together with the GROMOS96 43 A1 force field.[10,11] All runs focused on the dynamics of the β-heptapeptide H-β^3-HVal-β^3-HAla-β^3-HLeu-(*S*,*S*)-β^3-HAla(αMe)-β^3-HVal-β^3-HAla-β^3-HLeu-OH (Figure 1) in methanol at 340 K and under an ambient pressure of 1 atm. In two of the runs, the viscosity of the solvent was reduced by scaling the mass of each atom of every methanol molecule, and the time-step of integration was halved to account for higher frequency motions induced by this change: the scaling factor for the simulation with solvent viscosity $\eta_{low} = {}^1/_3\eta_n$ was 0.1, leading to a change in solvent viscosity by a factor of $^1/_3$, and a time-step of 1 fs was used in this case; for the simulation with solvent viscosity $\eta_{vlow} = {}^1/_{10}\eta_n$ the scaling factor was 0.01, leading to a change in solvent viscosity by a factor of $^1/_{10}$; the time-step was 0.5 fs. In the simulation at normal solvent viscosity (η_n) a time-step of 2 fs was used. The molecular models and simulation parameters are those used in reference [12].

Technical specifications of the simulation set-up are as follows: Thermodynamic constraints of temperature and pressure were maintained by

weak coupling[13] to an external bath: the thermostat was set with a coupling time of 0.1 ps; the barostat with 0.5 ps. Forces of interaction were computed in a rectangular simulation cell by using periodic boundary conditions and the minimum image convention. Non-bonded interactions were computed by using a twin-range cut-off scheme with radii of 0.8 nm and 1.4 nm and updated after every five time-steps. Covalent bonds were kept rigid with a precision of 10^{-4} by using the procedure SHAKE.[14]

The initial structure of the peptide for all three simulations was the 3_1-helical fold. It was surrounded by 962 methanol molecules in a rectangular box, the dimensions of which were chosen so that the minimum distance from the peptide to the box wall was 1.4 nm in the starting configuration. In all runs the dimensions of the simulation cell were large enough to accommodate a fully extended conformation of the β-heptapeptide.

Analysis procedures: The same methods and procedure of analysis used to process the simulation data were employed for each run. First, each configuration of the trajectory generated during the simulation was compared to the helical NMR model configuration. This was done by performing a translational and then a least-squares rotational fit to that configuration, followed by computing the root-mean-square deviation (for both procedures, backbone atoms of all residues except the termini of the oligomer were used). With a "folding event" defined as an interval at the beginning of which the peptide remains "folded" (i.e., with RMSD less than or equal to the threshold value of 0.1 nm) for at least 20 ps and at the end of which it remains unfolded for at least 20 ps, the RMSD time series was processed to give a distribution of residence times and statistics of that distribution. Estimates of thermodynamic characteristics of the "folding–unfolding" equilibrium were deduced from these statistics: the equilibrium constant of the folding equilibrium was computed as the ratio of the fraction of time spent unfolded to the fraction of time spent folded; the free energy was computed as $-RT\ln K$ (in which R is the universal gas constant, T is the absolute temperature, and K is the equilibrium constant). The next stage in the analysis involved comparing, in a similar way to that described above, each configuration in the trajectory to all other configurations in the trajectory. The results of the last step can be represented as a symmetric square matrix of RMSD values. An estimate of the conformational distribution corresponding to the trajectory was constructed from the RMSD matrix by using a centroid clustering algorithm[7] that proceeds as follows: a criterion of configurational similarity is set (here, 0.1 nm was used) and is used to determine, for each configuration, the number of configurations that are similar to it; the configuration with the largest number of structural neighbours is taken as the centre of the first conformational cluster; this, and configurations similar to it, are then disregarded; this process is repeated until all configurations have been assigned to a cluster. This algorithm generates clusters whose central members have a RMSD of at least 0.1 nm. It also tends to give many clusters that contain just one member. These are not necessarily conformations that were sampled once during the run: there may be configurations similar to them that lie just within other clusters.

Acknowledgements

We thank Xavier Daura for his support when initiating this study. Financial support from the National Center of Competence in Research (NCCR) in Structural Biology of the Swiss National Science Foundation is gratefully acknowledged.

[1] S. Yedgar, C. Tertreau, B. Gavish, D. Lavalette, *Biophys. J.* **1995**, *68*, 665–670.
[2] R. Walser, W. F. van Gunsteren, *Proteins: Struct. Funct. Genet.* **2001**, *42*, 414–421.
[3] R. Walser, A. E. Mark, W. F. van Gunsteren, *Chem. Phys. Lett.* **1999**, *303*, 583–586.
[4] R. Walser, B. Hess, A. E. Mark, W. F. van Gunsteren, *Chem. Phys. Lett.* **2001**, *334*, 337–342.
[5] B. Zagrovic, V. S. Pande, *J. Comput. Chem.* **2003**, *24*, 1432–1436.
[6] D. Seebach, P. E. Ciceri, M. Overhand, B. Jaun, D. Rigo, L. Oberer, U. Hommel, R. Amstutz, H. Widmer, *Helv. Chim. Acta* **1996**, *79*, 2043–2066.
[7] X. Daura, W. F. van Gunsteren, A. E. Mark, *Proteins: Struct. Funct. Genet.* **1999**, *34*, 269–280.
[8] H. A. Kramers, *Physica* **1940**, *7*, 284.
[9] W. R. P. Scott, P. H. Hünenberger, I. G. Tironi, A. E. Mark, S. R. Billeter, J. Fennen, A. E. Torda, P. Huber, P. Krüger, W. F. van Gunsteren, *J. Phys. Chem. A* **1999**, *103*, 3596–3607.
[10] W. F. van Gunsteren, S. R. Billeter, A. A. Eising, P. H. Hünenberger, P. Krüger, A. E. Mark, W. R. P. Scott, I. G. Tironi, *Biomolecular simulation: The GROMOS96 manual and user guide*, Vdf Hochschulverlag, Zürich, **1996**.
[11] X. Daura, A. E. Mark, W. F. van Gunsteren, *J. Comput. Chem.* **1998**, *19*, 535–547.
[12] X. Daura, W. F. van Gunsteren, D. Rigo, B. Jaun, D. Seebach, *Chem. Eur. J.* **1997**, *3*, 1410–1417.
[13] H. J. C. Berendsen, J. P. M. Postma, W. F. van Gunsteren, A. DiNola, J. R. Haak, *J. Chem. Phys.* **1984**, *81*, 3684–3690.
[14] J. P. Ryckaert, G. Ciccotti, H. J. C. Berendsen, *J. Comput. Phys.* **1977**, *23*, 327–341.

Received: May 26, 2005
Published online: October 31, 2005

